Toward an understanding of discrete ambiguities in truncated partial-wave analyses

Y. Wunderlich,[1] A. Švarc,[2] R. L. Workman,[3] L. Tiator,[4] and R. Beck[1]
[1]*Helmholtz-Institut für Strahlen- und Kernphysik der Universität Bonn, Nussallee 14-16, 53115 Bonn, Germany*
[2]*Rudjer Bošković Institute, Bijenička cesta 54, P.O. Box 180, 10002 Zagreb, Croatia*
[3]*Data Analysis Center at the Institute for Nuclear Studies, Department of Physics, George Washington University, Washington, D.C. 20052, USA*
[4]*Institut für Kernphysik, Universität Mainz, D-55099 Mainz, Germany*
(Received 7 September 2017; published 7 December 2017)

It is well known that the observables in a single-channel scattering problem remain invariant once the amplitude is multiplied by an overall energy- and angle-dependent phase. This invariance is called the continuum ambiguity and acts on the infinite partial-wave set. It has also long been known that, in the case of a truncated partial wave set, another invariance exists, originating from the replacement of the roots of partial-wave amplitudes with their complex conjugate values. This discrete ambiguity is also known as the Omelaenko-Gersten-type ambiguity. In this paper, we show that for scalar particles, discrete ambiguities are just a subset of continuum ambiguities with a specific phase and thus mix partial waves, as the continuum ambiguity does. We present the main features of both continuum and discrete ambiguities and describe a numerical method which establishes the relevant phase connection.

DOI: 10.1103/PhysRevC.96.065202

I. INTRODUCTION

In this work, we will consider the simple case of a $2 \to 2$ reaction amplitude $A(W,\theta)$ for scalar particles. We make this choice for illustrative and pedagogical purposes. The amplitude has the conventional partial-wave expansion

$$A(W,\theta) = \sum_{\ell=0}^{\infty}(2\ell+1)A_{\ell}(W)P_{\ell}(\cos\theta). \qquad (1)$$

The extraction of partial waves from data shall be studied, with data given in the case of the scalar reaction just by the differential cross section, which is defined as the modulus squared of $A(W,\theta)$ (ignoring explicit phase-space factors)

$$\sigma_0(W,\theta) = |A(W,\theta)|^2. \qquad (2)$$

Taking the positive branch of the square root on both sides of this equation, it is seen that at each point (W,θ) in phase space, the cross section confines the amplitude to a circle in the complex plane: $|A(W,\theta)| = +\sqrt{\sigma_0}$. Figure 1 shows a depiction of this fact. From the geometrical depiction as well as from the mathematical form of (2), it is quickly seen that the cross section remains unchanged under a rotation of the amplitude $A(W,\theta)$ by a phase, which is generally allowed to depend on energy and angle (see Fig. 1):

$$A(W,\theta) \to \tilde{A}(W,\theta) := e^{i\Phi(W,\theta)}A(W,\theta). \qquad (3)$$

The invariance under such transformations has long been well known and is generally referred to as the *continuum ambiguity* [1].

A different kind of ambiguity arises whenever the amplitude $A(W,\theta)$ has a zero in the angular variable, for instance, in $\cos\theta$ [2]. This can be seen by splitting the original amplitude $A(W,\theta)$ into the product of the linear factor belonging to the complex zero α, times a reduced amplitude $\hat{A}(W,\theta)$:

$$A(W,\theta) = \hat{A}(W,\theta)(\cos\theta - \alpha). \qquad (4)$$

When writing the differential cross section for this case, i.e.,

$$\sigma_0 = |\hat{A}(W,\theta)|^2(\cos\theta - \alpha^*)(\cos\theta - \alpha), \qquad (5)$$

it is evident that the complex conjugation of α, i.e., $\alpha \to \alpha^*$, does not change this observable. Since α is an angular zero, it has to be connected to the partial-wave amplitudes in some way. Thus, by leaping from one value of α to another one α^*, one achieves the same effect in the amplitude space. This means one transitions to a discretely diconnected point in this space, which yields the exact same cross section. In this way, these so-called *discrete ambiguities* acquire their name and they are a most prominent (but not fully exclusive) feature of truncated partial-wave analyses (TPWAs). The latter term refers to any analysis that involves a truncation of the infinite series (1) at some angular momentum L. With this knowledge, also the name continuum ambiguity given to the general rotations (3) can be understood. As it turns out [1], the vast size of this class of symmetry transformations, owing to the fact that they can be performed with in principle any function $\Phi(W,\theta)$, makes it possible to trace out connected arcs or even whole regions in amplitude space, which all have the same cross section. In fact, quite involved and sophisticated studies have been done in the past, in order to estimate and calculate such ambiguity continua [3]. Figure 2 gives a schematic illustration of the different types of ambiguites in partial-wave analyses. In this work, we investigate both continuum and discrete ambiguities as purely mathematical phenomena, which occur once partial waves are to be extracted from the quadratic form defined by the cross section (2). We will compare the large class of symmetry transformations generated by the general rotations (3), to the smaller class of discrete symmetries caused by root conjugation and elaborate how and under which circumstances traces of the latter class can be found in the former. The amount of ambiguity encountered may, of course, be reduced by introducing further physical constraints into the analysis, the most prominent one being the unitarity

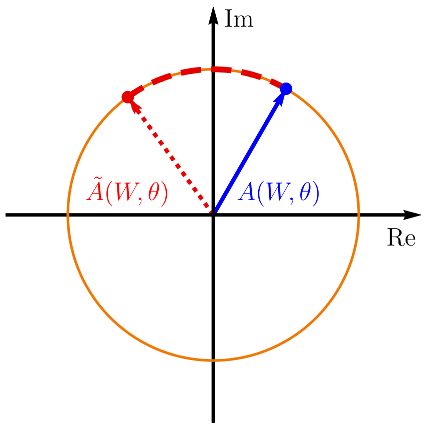

FIG. 1. The geometrical picture of the general continuum ambiguity (3) is depicted here. The differential cross section (2) constrains the true solution for the amplitude $A(W,\theta)$ (blue solid arrow) to be located on a circle of radius $+\sqrt{\sigma_0}$ in the complex plane (thin orange-colored circle). A rotation of the amplitude $A(W,\theta)$ to $\tilde{A}(W,\theta)$ (red dashed arrow and thick dashed curved line) does not alter the cross section.

of the $\hat{S}$ matrix [1]. We do not further pursue ambiguities under unitarity constraints here but leave them as a further avenue of exploration. It should just be mentioned that TPWAs performed below the first inelastic channel, where elastic unitarity is a very powerful contraint, are known to have discrete ambiguites,

so-called Crichton ambiguities [4]. The explorations of continuum ambiguities by Atkinson *et al.* [3] have also been performed under quite strict unitarity constraints.

We focus on the scalar amplitudes in order to keep the discussion as simple and illustrative as possible. However, it should be stated that the obtained results often carry over to analyses of more complicated reactions involving particles with spin (πN scattering, photoproduction), in many cases without large modifications.[1] Therefore, what is discussed here may also turn out to be relevant in recently initiated programs on analyses of so-called *complete* sets of polarization-data, performed for the spin reactions (see, for instance, Refs. [5–7]). This work is complementary to the study of Švarc *et al.* [8], which deals with related issues of ambiguities in partial-wave analyses.

II. CONTINUUM AMBIGUITIES AND THE MIXING FORMULA

Here, we consider continuum ambiguities, i.e., new partial-wave solutions generated by transforming the original amplitude $A(W,\theta)$ as in Eq. (3), using a general energy- and angle-dependent phase rotation $e^{i\Phi(W,\theta)}$. We choose to write the latter as a Legendre series:

$$e^{i\Phi(W,\theta)} = \sum_{k=0}^{\infty} L_k(W) P_k(\cos\theta). \tag{6}$$

As mentioned in the introduction, quite a lot of work has been done in the past on the capability of such rotations, which themselves have infinitely many real degrees of freedom, to generate ambiguous partial-wave solutions. Here, we want

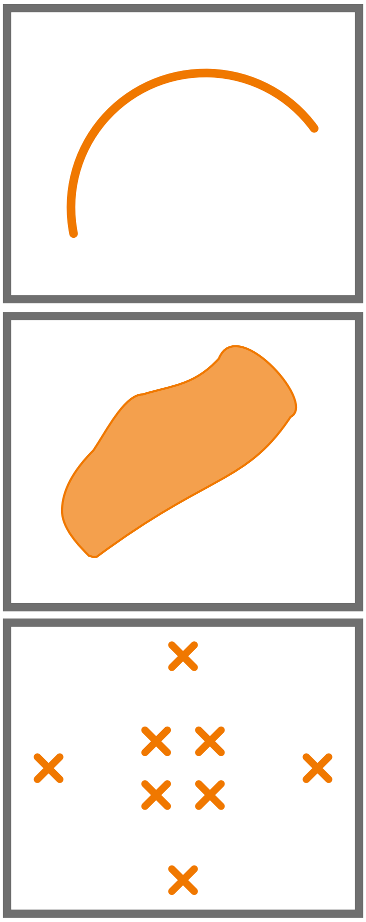

FIG. 2. Three schematics are shown in order to illustrate the meaning of the terms *discrete* and *continuum* ambiguities. The gray-colored box represents in each case the higher dimensional space furnished by the partial-wave amplitudes, be it for infinite partial-wave models or for truncated ones. Top: One-dimensional (for instance circular) arcs can be traced out by continuum ambiguity transformations, both for infinite and truncated models. Center: More general connected continua in amplitude space, containing an infinite number of points belonging to the same cross section, can be generated by use of the continuum ambiguity (3). However, this phenomenon is only present once the partial-wave series goes to infinity. The connected patches are also referred to as *islands of ambiguity* [1,3]. Bottom: Discrete ambiguities refer to cases where the cross section is the same for disconnected, discretely located points in amplitude space. These ambiguities are most prominent in TPWAs [1,14] (see Sec. III below). However, twofold discrete ambiguities can also appear for infinite partial-wave models, where elastic unitarity is employed [1].

[1] Some possible complications for the generalization to spin reactions are hinted at in the conclusions of this work.

to focus only on one aspect of the problem, namely the transformation of the original partial waves A_ℓ into waves $\tilde{A}_\ell$ belonging to the rotated amplitude $\tilde{A}(W,\theta)$, caused by the rotation (6). In the following derivation, we employ the notation $x = \cos\theta$. The projection integral for the transformed waves becomes

$$\begin{aligned} \tilde{A}_\ell(W) &= \frac{1}{2}\int_{-1}^{1} dx\, \tilde{A}(W,x) P_\ell(x) \\ &= \frac{1}{2}\int_{-1}^{1} dx\, e^{i\phi(W,x)} A(W,x) P_\ell(x) \\ &= \frac{1}{2}\int_{-1}^{1} dx \sum_{k=0}^{\infty} L_k(W) P_k(x) A(W,x) P_\ell(x) \\ &= \sum_{k=0}^{\infty} L_k(W)\, \frac{1}{2}\int_{-1}^{1} dx\, A(W,x) P_k(x) P_\ell(x), \end{aligned} \tag{7}$$

where in the last step, the permutation of the integral and the infinite k sum was just assumed to be valid. The product of Legendre polynomials under the integral in (7) is again expandable into the basis of Legendre polynomials. The resulting formula is known from the theory of the rotation group and can be written using either the Wigner $3j$ symbols or the well-known Glebsch-Gordan coefficients [9]:

$$\begin{aligned} P_k(x) P_\ell(x) &= \sum_{m=|k-\ell|}^{k+\ell} \begin{pmatrix} k & l & m \\ 0 & 0 & 0 \end{pmatrix}^2 (2m+1) P_m(x) \\ &= \sum_{m=|k-\ell|}^{k+\ell} \langle k,0;\ell,0|m,0\rangle^2 P_m(x). \end{aligned} \tag{8}$$

For the remainder of this work, the Clebsch-Gordan coefficients $\langle k,0;\ell,0|m,0\rangle$ are utilized. Using this recoupling formula, the partial-wave projection (7) becomes

$$\begin{aligned} \tilde{A}_\ell(W) &= \sum_{k=0}^{\infty} L_k(W)\, \frac{1}{2}\int_{-1}^{1} dx\, A(W,x) \\ &\quad \times \sum_{m=|k-\ell|}^{k+\ell} \langle k,0;\ell,0|m,0\rangle^2 P_m(x) \\ &= \sum_{k=0}^{\infty} L_k(W) \sum_{m=|k-\ell|}^{k+\ell} \langle k,0;\ell,0|m,0\rangle^2 \\ &\quad \times \frac{1}{2}\int_{-1}^{1} dx\, A(W,x) P_m(x) \\ &= \sum_{k=0}^{\infty} L_k(W) \sum_{m=|k-\ell|}^{k+\ell} \langle k,0;\ell,0|m,0\rangle^2 A_m(W). \end{aligned} \tag{9}$$

We see that the final result on the right-hand side takes the form of a linear combination, or mixing, of the partial waves $A_\ell(W)$ from the original amplitude. The precise form of the mixing is of course dictated by the energy-dependent Legendre coefficients $L_k(W)$ that define the phase rotation (6). Since this mixing formula is vital to the remainder of this work, we state it again in closed form:

$$\tilde{A}_\ell(W) = \sum_{k=0}^{\infty} L_k(W) \sum_{m=|k-\ell|}^{k+\ell} \langle k,0;\ell,0|m,0\rangle^2 A_m(W). \tag{10}$$

The general relation given in Eq. (10) has been derived using straightforward algebra and identities involving the Legendre polynomials. After this study was completed, we became aware of a paper by Dedonder *et al.* [10], which derives and states a similar mixing formula, however, for the special case of a phase $\Phi(W,\theta)$ linear in the Mandelstam variable $t = -2k^2(1-\cos\theta)$. We have not found the mixing formula in the general form (10) reproduced in the literature. For reactions involving particles with spin, on the other hand, similar mixing phenomena have been found either derived explicitly, or at least hinted at. Dean and Lee [11] give a very detailed treatment of analogous relations for πN scattering. Omelaenko [12] hints, near the end of his famous paper on discrete ambiguities in photoproduction, at similar circumstances for this particular reaction. Angle-dependent phase rotations and their effects in photoproduction are also discussed by Keaton and Workman [13]. Some mathematical comments on the mixing formula (10) are in order. First of all, angle-independent phase rotations are defined only by the lowest Legendre coefficient $L_0(W)$, with all higher ones vanishing [see Eq. (6)]. The mixing formula immediately tells that for these purely energy-dependent rotations, no mixing occurs at all and all partial waves are rotated by the same angle. However, once the continuum ambiguity phase $\Phi(W,\theta)$ has at least some angular dependence, the Legendre expansion (6) regains the full complexity of an infinite series. However, it is indeed feasible to construct phase rotations whose Legendre series converges rather quickly. In fact, for most examples considered in this work, they do. However, the mixing formula (10) then implies that for any angle dependence of the continuum ambiguity, mixing of partial waves necessarily occurs and furthermore is defined by an infinite tower of strictly speaking nonvanishing Legendre coefficients $L_k(W)$. Having discussed the effect of the general continuum ambiguity transformations on partial waves, we now introduce discrete ambiguities proper and outline the way in which they leave traces in the former, larger class of symmetry transformations.

III. DISCRETE AMBIGUITIES IN TPWAS AND GENERATING PHASE ROTATIONS

Next we consider TPWAs, i.e., those based on the partial wave series (1) cut off at some maximal angular momentum L. Gersten [14] has first noted the usefulness of decomposing such polynomial amplitudes into the product over their linear factors, i.e., by writing

$$\begin{aligned} A(W,\theta) &= \sum_{\ell=0}^{L} (2\ell+1) A_\ell(W) P_\ell(\cos\theta) \\ &\equiv \lambda \prod_{i=1}^{L} (\cos\theta - \alpha_i), \end{aligned} \tag{11}$$

where the α_i are a set of L complex zeros defining the amplitude. The complex normalization factor λ is, in the convention chosen above, proportional to the highest partial wave: $\lambda \propto A_L$. Furthermore, since the differential cross section (2) is a modulus squared, even in the truncated PWA, one energy-dependent overall phase has to be fixed prior to fitting the model (11) to data. One common choice could be to require the S wave to be real and positive: $A_0 = \mathrm{Re}[A_0] > 0$. This is the convention we will adhere to later. However, one could also choose to fix the normalization λ in (11) to be real, thereby also implying the same convention for the highest wave A_L. As mentioned in the introduction, the complex conjugation of a zero of any, either truncated or even infinite, partial-wave expansion generates a discrete ambiguity. Since in the truncated case, the amplitude (11) is nothing but a product over linear factors, the cross section

$$\sigma_0 = |\lambda|^2 \prod_{i=1}^{L} (\cos\theta - \alpha_i^*)(\cos\theta - \alpha_i) \tag{12}$$

is unchanged by all possibilities of conjugating subsets of roots [14]. There exist in total 2^L such possibilities and we adhere to the formalization of all those possibilities introduced by Gersten [14]. Therefore, we define a set of 2^L maps

$$\boldsymbol{\pi}_p(\alpha_i) := \begin{cases} \alpha_i & , \mu_i(p) = 0 \\ \alpha_i^* & , \mu_i(p) = 1 \end{cases}, \tag{13}$$

where the binary representation of the number p,

$$p = \sum_{i=1}^{L} \mu_i(p) 2^{(i-1)}, \tag{14}$$

has been employed. The index p just labels all combinatorically possible ambiguities acting on the roots α_i, with $\boldsymbol{\pi}_0$ being the identity. Now, it is easy to define ambiguity-transformed truncated amplitudes $A^{(p)}(W,\theta)$ which, since the number of factors in (11) is unchanged by any of the Gersten ambiguities (13), retains the same truncation order L as the original amplitude

$$\begin{aligned} A^{(p)}(W,\theta) &= \lambda \prod_{i=1}^{L} (\cos\theta - \boldsymbol{\pi}_p[\alpha_i]) \\ &\equiv \sum_{\ell=0}^{L} (2\ell+1) A_\ell^{(p)}(W) P_\ell(\cos\theta). \end{aligned} \tag{15}$$

The ambiguous amplitudes $A^{(p)}$ have the same cross section as the original model A. According to remarks made in the introduction, this means that they have to be connected to the original amplitude by rotations (see Fig. 1). These phase rotations are, once the Gersten formalism has been established, computed without effort:

$$\begin{aligned} e^{i\varphi_p(W,\theta)} &= \frac{A^{(p)}(W,\theta)}{A(W,\theta)} \\ &= \frac{(\cos\theta - \boldsymbol{\pi}_p[\alpha_1]) \ldots (\cos\theta - \boldsymbol{\pi}_p[\alpha_L])}{(\cos\theta - \alpha_1) \ldots (\cos\theta - \alpha_L)}. \end{aligned} \tag{16}$$

Remembering the definition of the maps (13), it can be seen quickly that the resulting expression has modulus 1 for all $\cos\theta \in [-1,1]$, as it should. Some more remarks have to be made about the result (16). First of all, for all ambiguities except the identity $\boldsymbol{\pi}_0$ (which leads to $e^{i\varphi_0(W,\theta)} = 1$), the phase rotation is explicitly angle dependent. As mentioned in Sec. II, a purely energy-dependent phase rotation rotates all partial waves by the same angle. The discrete Gersten ambiguities have a different nature, leading via the conjugations of the roots α_i to more intricate transformations on the level of partial waves A_ℓ. Already for low truncation orders L, conjugations of single waves can be observed, or more generally rotations of different waves by different angles. In order to achieve this, the generating phase rotations (16) have to have at least some angle dependence. Second, in establishing the discrete Gersten ambiguities to be generated by phase rotations (16), a connection has been drawn between the discrete partial-wave ambiguities discussed in this section and the more general continuum ambiguities treated in Sec. II. In particular, since the generating phases (16) are angle dependent, they have, by means of Eq. (10) above, to lead to partial-wave mixing. In any case, an angle-dependent phase has an infinite Legendre expansion. However, from their definition the phases (16) again lead to manifestly truncated amplitudes (15). Therefore, these generating phase rotations are finely tuned such that they lead to exact cancellations on the right-hand side of the mixing formula (10), for all $\ell > L$.

Gersten [14] stated, without proof, that the transformations (13) exhaust all possibilities to form discrete ambiguities in a TPWA. To be more precise, he mentions a further discrete symmetry, namely

$$A^{(p)}(W,\theta) \longrightarrow -\left[A^{(p)}(W,\theta)\right]^*, \tag{17}$$

which has, however, been removed by fixing a suitable phase convention in the analysis, requiring one specific partial wave (for instance, A_0) to be real and positive. We have to state that we consider Gersten's claim to be true. There really are no more ways to transform to disconnected points in amplitude space where the truncated PWA model is ambiguous. However, having reformulated the Gersten ambiguities in a language that fits the general continuum ambiguities of Sec. II, we would like to reformulate the claim in a different guise:

The phase rotations $e^{i\varphi_p(W,\theta)}$ form a discrete subclass of the general continuum ambiguity phases $e^{i\Phi(W,\theta)}$, representing all possible phase rotations capable of rotating the original truncated amplitude $A(W,\theta)$ again into a truncated one. Thus, all the remaining infinite rotations contained in the larger class of symmetries $e^{i\Phi(W,\theta)}$ produce rotated models which are no longer truncated at L. The generating phases $e^{i\varphi_p(W,\theta)}$ are fully exhaustive in their capability to produce truncated models out of continuum ambiguity transformations.

Like Gersten, we do not have a precise mathematical proof of this claim. However, in the next section a numerical method is introduced capable of substantiating what has been stated above.

IV. FUNCTIONAL MINIMIZATION FORMALISM AND THE EXHAUSTIVENESS OF THE GERSTEN AMBIGUITIES

In the following, we again employ the notation $x = \cos\theta$. Furthermore, since phase rotations [such as those in Eq. (16)] will have to be searched numerically in what is to come, we switch from working with the phases themselves directly to the complex rotation functions

$$F(W,x) := e^{i\Phi(W,x)}. \tag{18}$$

Using the rotations has several advantages. Mainly, equations such as (16) only fix the phases $\Phi(W,x)$ themselves up to the branch-point singularity of the logarithm, which has to be encountered once the exponential is inverted. One could fix a convention, such as choosing the principal branch of the logarithm for the phases. Usage of the rotation functions circumvents this problem altogether. In the following, we will sometimes loosely refer to the concept of vector spaces of functions. However, observe that the functions $F(W,x)$ do not form a vector space, since they do not close under addition and scalar multiplication. The functions $\Phi(W,x)$, on the other hand, do. From now on, we consider the action of the rotation (18) in a general continuum ambiguity transformation (3), i.e., $A(W,x) \rightarrow \tilde{A}(W,x) = F(W,x)A(W,x)$. The amplitude $A(W,x)$ is truncated at L and a known input. In order to look for Gersten-type ambiguities, or potential further symmetries with similar properties, we solve the following two constraints at a fixed energy W:

(I) The rotated amplitude $\tilde{A}$, coming out of an amplitude A truncated at L, has to be truncated as well, i.e.,

$$\tilde{A}_{L+k}(W) = 0, \ \forall k = 1,\ldots,\infty. \tag{19}$$

(II) The complex solution function $F(W,x)$ has to have modulus 1 for each value of x:

$$|F(W,x)|^2 = 1, \ \forall x \in [-1,1]. \tag{20}$$

The problem proposed here is a problem from functional analysis (or functional problem for short), since one tries to scan a full vector space of functions $\Phi(W,x)$ [implied up to logarithmic singularities by our solutions $F(W,x)$], for solutions of the problem. The obtained complex function is a solution to the infinite set of functional equations

$$\tilde{A}_{L+k}(W) = \frac{1}{2}\int_{-1}^{+1} dx F(W,x)A(W,x)P_{L+k}(x) \equiv 0, \quad \forall\, k = 1,\ldots,\infty. \tag{21}$$

This set of equations corresponds to the formal statements of the functional problem we are trying to solve. However, it has to be clear that for any practical numerical calculation, an equation system built out of infinitely many functionals can never be solved. Therefore, in all practical examples we impose a restriction on the index k, making it range up to some finite, but sufficiently large, value K_{cut}:

$$k = 1,\ldots,K_{\text{cut}}. \tag{22}$$

Now, we formally define a quantity which, through its minimization, allows for the solution of conditions (I) and (II) above. Also, due to the length of some of the ensuing expressions, explicit energy dependences are in most cases implicit. The quantity to be minimized reads

$$\begin{aligned}\boldsymbol{W}[F(x)] := &\sum_x (\text{Re}[F(x)]^2 + \text{Im}[F(x)]^2 - 1)^2 \\ &+ \text{Im}\left[\frac{1}{2}\int_{-1}^{+1} dx\, F(x)A(x)\right]^2 \\ &+ \sum_{k\geqslant 1}\left\{\text{Re}\left[\frac{1}{2}\int_{-1}^{+1} dx\, F(x)A(x)P_{L+k}(x)\right]^2\right. \\ &\left. + \text{Im}\left[\frac{1}{2}\int_{-1}^{+1} dx\, F(x)A(x)P_{L+k}(x)\right]^2\right\}. \end{aligned}\tag{23}$$

This $\boldsymbol{W}[F(x)]$ maps any whole phase-rotation function $F(x)$ to a real number. Therefore, it is also formally a functional. The individual terms in the minimization functional (23) implement all the required constraints on the rotation function $F(x)$. Minimization of the first term in the first line makes the function unimodular, cf. constraint (II) above. The sum $\sum_x$ is written in order to indicate that in any practical example, this term is evaluated on a discrete grid of equidistant points $\{x_n\} \in [-1,1]$ (more on this below). The term in the second line invokes an overall phase convention for the partial waves, by making the S wave A_0 real. However, note that it does not make the latter positive (as in the convention declared in Sec. III), such that additional sign ambiguities may be expected for the solutions. Finally, the third term filling the entire third and fourth line of Eq. (23) formally implements constraint (I) by setting all partial wave projections above $\tilde{A}_L$ to zero, once it adopts its minimum. In any practical minimization, the sum over k is truncated at some K_{cut} [see Eq. (22)]. We now come to the central statement of this section. We claim that once any suitable scheme for the minimization of the functional $\boldsymbol{W}[F(x)]$ is applied, then those minima consistent with zero up to a good numerical approximation will yield as solutions only the discrete Gersten ambiguities. This can be written in idealized form as

$$\boldsymbol{W}[F(W,\theta)] \longrightarrow \text{min.} \equiv 0, \tag{24}$$

$$\text{for } F(W,\theta) \longrightarrow F_p(W,\theta) = e^{i\varphi_p(W,\theta)}, \quad p = 0,\ldots,(2^L - 1). \tag{25}$$

Of course, as mentioned below Eq. (23), an additional sign ambiguity exists due to the fact that the S wave is only fixed to be real, but not positive, in our definition of $\boldsymbol{W}[F(x)]$. However, such sign ambiguities can be resolved easily, once the minimization has been performed. Any numerical scheme used to find general minima, or solution functions, from the minimization of (23) needs to implement some method to parametrize the functions $F(x)$ as generally as possible. Here, we employ a Legendre expansion

$$F(\{y_{\ell'},w_{\ell'}\})(x) := \sum_{\ell'=0}^{\mathcal{L}_{\text{cut}}}(y_{\ell'} + i w_{\ell'})P_{\ell'}(x) \equiv \sum_{\ell'=0}^{\mathcal{L}_{\text{cut}}} L_{\ell'} P_{\ell'}(x), \tag{26}$$

with $y_{\ell'} = \mathrm{Re}[L_{\ell'}]$ and $w_{\ell'} = \mathrm{Im}[L_{\ell'}]$. The latter are the parameters for which to solve. The expansion (26) becomes numerically tractable with a truncation at some, possibly large, expansion index $\mathcal{L}_{\mathrm{cut}}$.[2] Since the partial waves A_ℓ of the nonrotated amplitude are assumed to be known, one can directly use the mixing formula (10) in order to parametrize the rotated partial waves $\tilde{A}_\ell$ (above L) in terms of the minimization parameters $y_{\ell'}$ and $w_{\ell'}$. This has the advantage of avoiding the need to explicitly implement numerical integration into the minimization routine. However, the mixing formula as used here is slightly modified due to two facts: First of all, the original amplitude is truncated at L, and second, the Legendre expansion of the phase rotation is cut off at $\mathcal{L}_{\mathrm{cut}}$. The result reads

$$\tilde{A}_{L+k}(\{y_{\ell'},w_{\ell'}\}) = \sum_{\ell'=k}^{\min(2L+k,\mathcal{L}_{\mathrm{cut}})} (y_{\ell'} + i w_{\ell'}) \times \sum_{m=|L+k-\ell'|}^{L} \langle \ell',0;\ell,0|m,0\rangle^2 A_m, \ \ \forall\, k = 1,\ldots,K_{\mathrm{cut}}. \tag{27}$$

This expression implies that in the chosen ansatz for the functional minimization, the maximal index $\mathcal{L}_{\mathrm{cut}}$ sets a limit on the parameter K_{cut}. The maximal choice, which we always use in the following, is

$$K_{\mathrm{cut}} = \mathcal{L}_{\mathrm{cut}}. \tag{28}$$

The minimization scheme based on the Legendre parametrization (26) and the mixing formula (27) has turned out to be quite well behaved numerically. Another, less favorable, ansatz for the parametrization of $F(x)$ consists of using a discretization of this function for a discrete set of values $\{x_n\} \in [-1,1]$. We briefly summarize this alternative procedure in Appendix A but do not utilize it further in the main discussion. Since the first term in the functional (23) features a summation over x in any case, a discrete grid of points $\{x_n\} \in [-1,1]$ is needed for the Legendre ansatz as well. We employ a total number of N_I equidistant points with separation

$$\Delta x = \frac{1-(-1)}{N_I} = \frac{2}{N_I}. \tag{29}$$

To define this sequence of base points, a simple prescription is used:

$$x_n := -1 + \left(\frac{1+2(n-1)}{2}\right)\Delta x. \tag{30}$$

[2]Angle-dependent rotations are always, strictly speaking, infinite expansions in x (see Sec. II). However, in practical cases it is clearly impossible to solve for infinitely many Legendre coefficients. With the finite expansion, we want to simulate a convergent infinite series. For practical examples, $\mathcal{L}_{\mathrm{cut}}$ has to be chosen much larger than the order for which the calculable Gersten phases already achieve a good convergence. Then, this ansatz works numerically, as illustrated by the example below.

The points therefore make up the set

$$x_n \in \left\{\frac{\Delta x}{2} - 1, \ldots, \left[\frac{1+2(N_I-1)}{2}\right]\Delta x - 1\right\}. \tag{31}$$

Using the definitions (26), (27), and (30), as well as the fact that the truncation order L and partial waves A_ℓ of the original amplitude are known input, the functional $\boldsymbol{W}[F(x)]$ can be written as an ordinary function depending on the parameters $\{y_{\ell'},w_{\ell'}\}$. The result, which is then optimized in the Legendre ansatz, becomes

$$\begin{aligned} \boldsymbol{W}_{\mathcal{L}}(\{y_{\ell'},w_{\ell'}\}) &:= \sum_{\{x_n\}} (\mathrm{Re}[F(\{y_{\ell'},w_{\ell'}\})(x_n)]^2 \\ &\quad + \mathrm{Im}[F(\{y_{\ell'},w_{\ell'}\})(x_n)]^2 - 1)^2 + \mathrm{Im}[\tilde{A}_0(\{y_{\ell'},w_{\ell'}\})]^2 \\ &\quad + \sum_{k=1}^{K_{\mathrm{cut}}} (\mathrm{Re}[\tilde{A}_{L+k}(\{y_{\ell'},w_{\ell'}\})]^2 + \mathrm{Im}[\tilde{A}_{L+k}(\{y_{\ell'},w_{\ell'}\})]^2). \end{aligned} \tag{32}$$

A useful feature of model-independent expansions into basis functions such as (26) is that once they are employed, complicated functionals become just ordinary functions depending on the expansion coefficients. The explicit mathematical form of the function (32) is elaborated in more detail in Appendix B, but for the ensuing discussion it is not really needed. An open question remains about which initial conditions for the $\{y_{\ell'},w_{\ell'}\}$ to choose for the minimization process. We employ an ensemble consisting of $N_{\mathrm{MonteCarlo}}$ sets of start parameters. How many to choose depends on the order L of the original truncated model. Mostly, we employed values around $N_{\mathrm{MonteCarlo}} = 50,\ldots,100$ for the treatment of simple toy-model examples, with generally satisfactory results. For the precise method to generate the $N_{\mathrm{MonteCarlo}}$ start configurations, we have made good experiences by just drawing each parameter randomly from the interval $[-1,1]$, for example by using RandomReal[{−1,1}] in MATHEMATICA. Also, all numerical minimizations shown in the following have been done with MATHEMATICA.

What remains to be done is to demonstrate the machinery presented in this section on a particular example. We consider a simple toy-model consisting of an amplitude truncated at $L = 2$, with partial waves given in arbitrary units:

$$\begin{aligned} A(x) &= \sum_{\ell=0}^{2} (2\ell+1) A_\ell P_\ell(x) \\ &= A_0 + 3A_1 P_1(x) + 5A_2 P_2(x) \\ &= 5 + 3(0.4 + 0.3i)x + \frac{5}{2}(0.02 + 0.01i)(3x^2 - 1). \end{aligned} \tag{33}$$

Note that in addition to the truncation, this model is constructed in such a way that the nonvanishing partial waves show a soft convergence behavior. Once the Gersten decomposition (11) is computed for this example, the following values for the complex normalization-factor

$$\lambda = 0.15 + 0.075i, \tag{34}$$

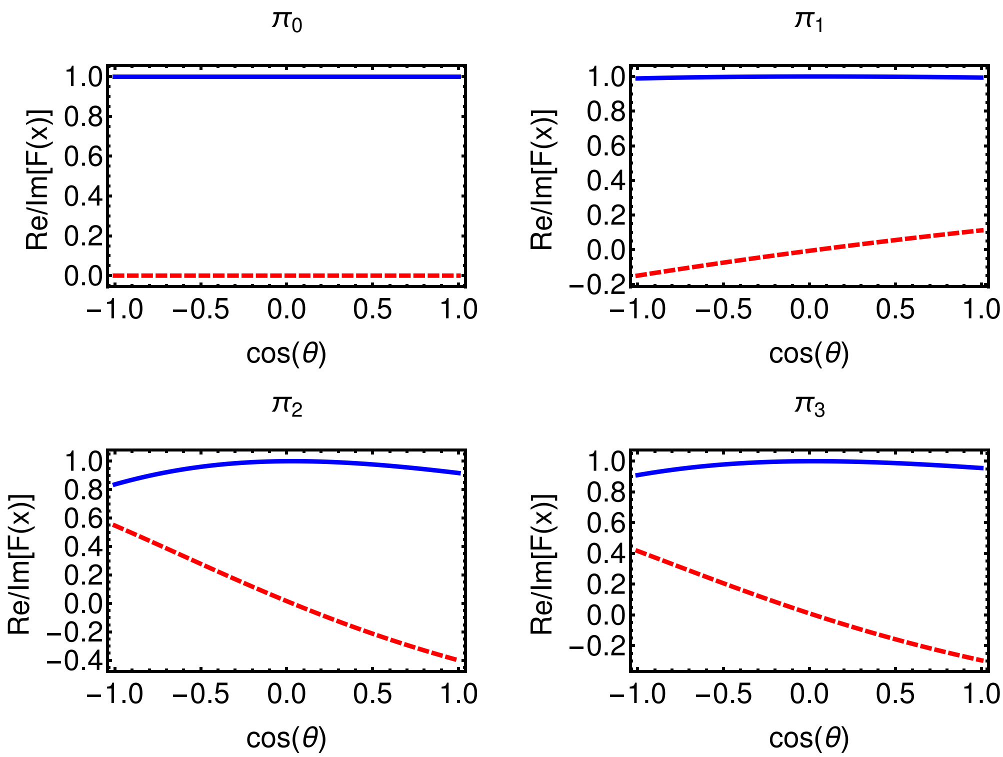

FIG. 3. These plots show the real (blue solid line) and imaginary parts (red dashed line) of the phase rotations (39) extracted from the toy-model amplitude (33) defined in the main text. The individual figures are labeled via the respective ambiguity $\boldsymbol{\pi}_p$ belonging to each phase $e^{i\varphi_p(x)}$.

as well as the two roots

$$\alpha_1 = -7.05858 - 4.63163i, \tag{35}$$

$$\alpha_2 = -1.74142 + 3.03163i, \tag{36}$$

are obtained. Since the toy model (33) is truncated at $L = 2$, there exist $2^2 = 4$ Gersten ambiguities, which according to Eqs. (13) and (14) are enumerated as follows:

$$\boldsymbol{\pi}_0(\alpha_1,\alpha_2) = (\alpha_1,\alpha_2), \quad \boldsymbol{\pi}_1(\alpha_1,\alpha_2) = (\alpha_1^*,\alpha_2), \tag{37}$$

$$\boldsymbol{\pi}_2(\alpha_1,\alpha_2) = (\alpha_1,\alpha_2^*), \quad \boldsymbol{\pi}_3(\alpha_1,\alpha_2) = (\alpha_1^*,\alpha_2^*). \tag{38}$$

The generating phases of the discrete ambiguities (37) and (38) can be evaluated using Eq. (16) from Sec. III. Four different rotations are obtained,

$$e^{i\varphi_0(x)} = 1,\ e^{i\varphi_1(x)},\ e^{i\varphi_2(x)},\ e^{i\varphi_3(x)}, \tag{39}$$

with all of them, except for the phase of the identity $\boldsymbol{\pi}_0$, depending on $x = \cos\theta$ (energy dependencies suppressed). The phase rotations (39) are plotted in Fig. 3 as complex functions of x. Their Legendre coefficients, up to and including L_8, are collected in Table I. Apart from the trivial dependence of $e^{i\varphi_0(x)}$, the remaining phase rotations $e^{i\varphi_1(x)}$, $e^{i\varphi_2(x)}$ and $e^{i\varphi_3(x)}$ show a relatively quick convergence. This makes the toy model (33) a well-suited example for the demonstration of the functional minimization formalism, since the range $\mathcal{L}_{\text{cut}}$ of the Legendre parametrization (26) can be chosen comparatively low, making the calculations numerically tractable. With

TABLE I. This table collects the Legendre coefficients of the phase rotations (39) corresponding to the toy-model amplitude (33) defined in the main text. All coefficients up to L_8 are shown. All numbers are printed to 5 significant digits, in order to illustrate the quick convergence of these examples.

L_k	$e^{i\varphi_0(x)}$	$e^{i\varphi_1(x)}$	$e^{i\varphi_2(x)}$	$e^{i\varphi_3(x)}$
L_0	1	$0.997 - 0.01049i$	$0.95864 + 0.03697i$	$0.97741 + 0.02781i$
L_1	0	$0.00182 + 0.13038i$	$0.02769 - 0.48277i$	$0.01563 - 0.35988i$
L_2	0	$-0.00581 - 0.00852i$	$-0.08227 + 0.03939i$	$-0.04507 + 0.03429i$
L_3	0	$0.00068 + 0.00028i$	$0.0126 + 0.009i$	$0.00769 + 0.00427i$
L_4	0	$-0.00005 + 9.6 \times 10^{-6}i$	$0.00029 - 0.00249i$	$0.00005 - 0.00148i$
L_5	0	$2.3 \times 10^{-6} - 2.3 \times 10^{-6}i$	$-0.00037 + 0.00015i$	$-0.00021 + 0.00011i$
L_6	0	$-4.4 \times 10^{-8} + 2.1 \times 10^{-7}i$	$0.00005 + 0.00004i$	$0.00003 + 0.00002i$
L_7	0	$-4.98 \times 10^{-9} - 1.3 \times 10^{-8}i$	$1.6 \times 10^{-6} - 9.1 \times 10^{-6}i$	$4.0 \times 10^{-7} - 5.5 \times 10^{-6}i$
L_8	0	$7.0 \times 10^{-10} + 4.9 \times 10^{-10}i$	$-1.3 \times 10^{-6} + 4.5 \times 10^{-7}i$	$-7.6 \times 10^{-7} + 3.5 \times 10^{-7}i$

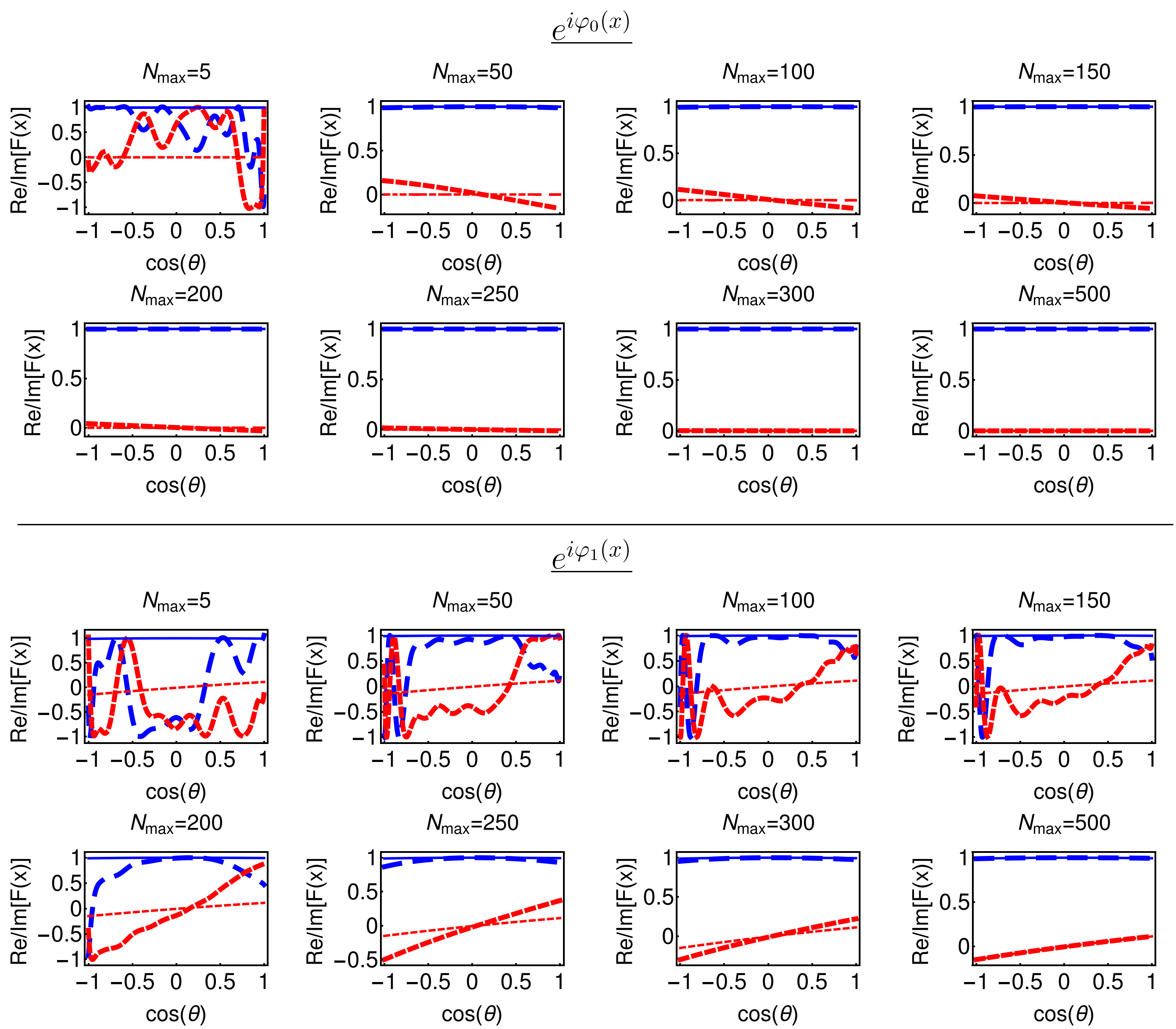

FIG. 4. The convergence process of the functional minimization procedure as described in the main text is demonstrated here. For the phase rotations $e^{i\varphi_0(x)}$ and $e^{i\varphi_1(x)}$, generating the discrete ambiguities $\boldsymbol{\pi}_0$ and $\boldsymbol{\pi}_1$ of the toy model (33), two randomly drawn initial functions have been picked from the applied ensemble. These initial conditions have, in the process of minimization, converged to these two respective phases. Minimizations have been performed by starting always at the same initial function, but applying different numbers for the maximal number of iterations $N_{\max}$ of the minimizer, as indicated in the headers of the plots. Values range from $N_{\max} = 5$ (minimizer has barely changed the initial function) up to $N_{\max} = 500$ (convergence condition fulfilled for any of the minimizations). In all plots, the real and imaginary parts of the precise Gersten ambiguity are drawn as thin blue solid lines and thin red finely dashed lines, respectively. The results of the functional minimizations up to $N_{\max}$ are drawn as thick blue coarsely dashed lines for the real parts and thick red finely dashed lines for the imaginary parts.

the toy model (33) as input, we performed a numerical minimization of the abstract functional (23). The Legendre parametrization (26) for the phase rotations was utilized, such that the procedure reduced to the optimization of the ordinary function (32), with the Legendre coefficients $\{y_{\ell'}, w_{\ell'}\}$ as free parameters of the problem. The truncation orders

$$\mathcal{L}_{\text{cut}} = K_{\text{cut}} = 20 \tag{40}$$

were employed. Minimizations started from an ensemble of $N_{\text{MonteCarlo}} = 50$ different initial parameter configurations. The angular interval $x \in [-1,1]$ has been divided into $N_I = 400$ equidistant points $\{x_n\}$. As a result of the functional minimization, we report that the anticipated exhaustiveness of the Gersten ambiguities, formulated generally in Eqs. (24) and (25) above, has been fully confirmed. In the case at hand, this fact may be briefly expressed as

$$\boldsymbol{W}_{\mathcal{L}}(\{y_{\ell'}, w_{\ell'}\}) \longrightarrow \text{min.} \equiv 0, \tag{41}$$

$$\text{for} \quad F(x) \longrightarrow e^{i\varphi_p(x)},\ p = 0, \ldots, 3. \tag{42}$$

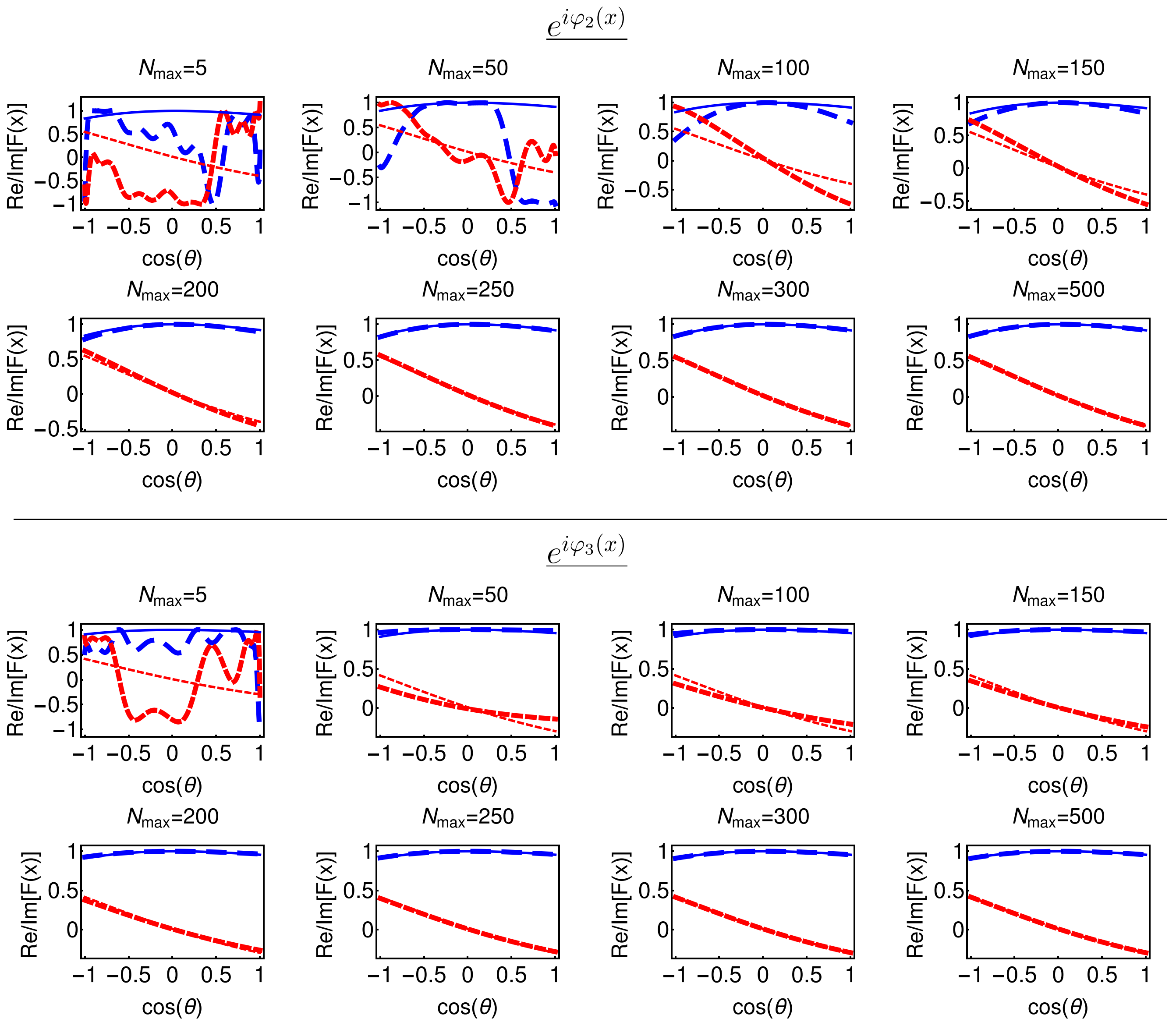

FIG. 5. This is the continuation of Fig. 4. Convergence of the minimization of the functional (23) is illustrated for the phases $e^{i\varphi_2(x)}$ and $e^{i\varphi_3(x)}$, which generate discrete symmetries for the toy model (33).

The consistency of the functional-minimum (41) with zero means in this practical numerical case that the values of the adopted minima range around $10^{-29},\dots,10^{-30}$. Local minima are found as well, but they are typically separated from the global (mathematical) minima by many orders of magnitude. They typically correspond to values of the order 1 for the functional. These results have not been modified by raising $N_{\mathrm{MonteCarlo}}$.

A graphical representation of the convergence process for the functional minimizations is provided in Figs. 4 and 5. There, four different randomly chosen initial functions have been picked, each of them leading to a different Gersten ambiguity in the process of minimization. Then, numerical minimizations have been performed for eight different ascending values of the maximal number of iterations $N_{\max}$. For the maximal value $N_{\max} = 500$, the minimizations have converged to the precise Gerten ambiguity in any case. However, apart from that, differences can be observed in the speed of convergence. The identity $e^{i\varphi_0(x)}$ and full conjugation ambiguity $e^{i\varphi_3(x)}$ are found most quickly via the optimization, while the ambiguities $e^{i\varphi_1(x)}$ and $e^{i\varphi_2(x)}$ require more iterations.

V. CONCLUSIONS AND OUTLOOK

Ambiguities in the extraction of partial waves for the scalar case have been the main focus of this work. Continuum ambiguities caused by general energy- and angle-dependent phase rotations, as well as discrete ambiguities stemming from the conjugation of zeros, have been formalized and compared. The discrete symmetries first defined by Gersten have been found to be a specific subclass of the larger symmetry group of continuum ambiguities, with the property that they fully exhaust all possibilities to rotate an original truncated amplitude again into a truncated one. This subclass is unique in the sense that no further transformations exist which can lead back to truncated models. Furthermore, the partial waves of the transformed amplitude have in all cases, i.e., for the full continuum ambiguity group as well as for the discrete symmetries, turned out to be mixings of the partial waves from the original amplitude. Since the discrete symmetries lead to truncated models again, they are finely tuned in such a way that exact cancellation occurs in all partial waves from the rotated model above the truncation order L.

In order to substantiate the above-mentioned exhaustiveness statement from a perspective which is orthogonal to the Gersten formalism, a straightforward and, as far as we know, new method has been introduced based on the numerical minimization of functionals. Such functionals allow for a flexible way to scan the infinitely possible phase-rotation functions $F(W,\theta) = e^{i\Phi(W,\theta)}$ for those obeying the implemented constraints, which in this case consisted of the vanishing of all transformed partial waves above L. First numerical tests for simple toy models yielded consistent results and have in all cases confirmed the exhaustiveness statement on the discrete ambiguities.

The present study is certainly just a beginning of further formal studies on partial-wave ambiguities. We list in the following a few interesting open questions as well as further avenues of investigation:

(i) The exhaustiveness, or uniqueness, property of the Gersten ambiguities has not been supported by a formal proof in this work. To perform this task, almost certainly a more sophisticated application of algebra or functional analysis will be needed. Still, a better mathematical understanding of the discrete ambiguities and why they appear may also lead to a better grasp of the process of partial-wave fitting and the quadratic equation systems involved.

(ii) A discrete class of angle-dependent phase rotations has been formulated capable of rotating all models with the same truncation order L into each other, i.e., of rotating $L \to L$. One may ask whether it is formally possible to raise the truncation order using angle-dependent phase rotations, i.e., to rotate truncations

$$L \to L + \mathbb{N}. \tag{43}$$

In the present case, the answer appears negative. However, it is not quite certain. Possibilities of changing truncation orders by phase rotations would in any case be interesting. The search for such phases may, for instance, be performed using ideas similar to the functional methods outlined in this work.

(iii) The study of ambiguities in this work did not impose unitarity constraints on the amplitude. It would certainly be interesting to see how to impose strict unitarity requirements using ideas similar to the functional minimization, or how to link the findings of this work to the residual Crichton ambiguities appearing below the first inelastic threshold.

(iv) Finally, the formal treatment of ambiguities presented here may be extended to reactions with spin or even with multiparticle final states. πN scattering has been treated in some detail in the past [11]. For photoproduction, no formal treatment of partial-wave mixing and continuum vs discrete ambiguites as presented in this work has been found. The functional methods developed here may also be extended to spin reactions.

However, a *word of warning* should be said about reactions with spin. The following statements stem from preliminary considerations done for πN scattering and for photoproduction of single pseudoscalar mesons, but may turn out to be more general, at least in the context of two-body reactions. It is well known that for such reactions the overall reaction amplitude can be parametrized in a model-independent way using N invariant amplitudes [15], where the integer N depends on the spins of the participating particles. Upon converting to the center-of-mass frame, different schemes of spin quantization can be used to obtain N so-called spin amplitudes. It is often convenient to use the basis of N transversity amplitudes $\{b_j(W,\theta), j = 1,\dots,N\}$. The latter shall be chosen in the following. In the case of πN scattering, for instance, there exist $N = 2$ amplitudes. Pseudoscalar meson photoproduction is described by $N = 4$ amplitudes. Once more than one amplitude is in the game, it is important to distinguish different types of continuum ambiguity transformations, or in other words, rotations. The first, most general, kind of transformation rotates every transversity amplitude b_j by a *different* phase ϕ_j and is thus referred to as an N-fold continuum ambiguity[3]

$$b_j(W,\theta) \to e^{i\phi_j(W,\theta)} b_j(W,\theta),\ j = 1,\dots,N. \tag{44}$$

This is a much larger class of symmetry transformations than the rotation of all amplitudes by the *same* phase Φ, from now on referred to as a 1-fold continuum ambiguity

$$b_j(W,\theta) \to e^{i\Phi(W,\theta)} b_j(W,\theta),\ j = 1,\dots,N. \tag{45}$$

From inspection of the well-known linear factor decompositions of the πN and photoproduction amplitudes [12,14], we have been able to infer that at least in these two cases, the Gersten-type ambiguities (i.e., those stemming from root conjugation) are in general generated by N-fold rotations (44) and *not* by the 1-fold ones (45).[4] Thus, the fact that discrete Gersten-type ambiguities fall into the general 1-fold rotations is a special feature only present for the scalar reactions, caused by the fact that there exists only one amplitude. For the more general cases with spin, one has to carefully distinguish which kind of symmetry is generated from which kind of rotation, and the generalization of the scalar results obtained in this work is by no means trivial.

The distinction of N- and 1-fold continuum ambiguities made here becomes interesting once one considers the observables measurable in a spin reaction. It is again well known

[3]We use here the language of Höhler [16], who discusses two-fold continuum ambiguities in the context of πN scattering.

[4]This fact has been observed only for the two example reactions. We just assume that it carries over to more general spin reactions.

that for two-body reactions, N^2 polarization observables $\mathcal{O}^a$ can be accessed, at least in principle [15]. When written in the transversity basis, there exists a subset of N observables given just by a sum of moduli squared of the amplitudes (proportionality in the following equation up to phase-space factors)

$$\mathcal{O}^a_{\boldsymbol{d}}(W,\theta) \propto \pm|b_1(W,\theta)|^2 \pm \cdots \pm |b_N(W,\theta)|^2, \quad (46)$$

for $a = 1,\ldots,N$. The signs in front of each squared amplitude depend on the observable and conventions used. When considered as a bilinear form of the amplitudes, the N observables $\mathcal{O}^a_{\boldsymbol{d}}$ are defined by diagonal matrices (thus the subscript $\boldsymbol{d}$). For πN scattering, the diagonal observables would be the unpolarized cross section σ_0 and the target-polarization asymmetry $\hat{P}$ [11,16]. In case of photoproduction, it is well known that the single-spin observables σ_0, $\hat{\Sigma}$, $\hat{T}$, and $\hat{P}$ are diagonal [12,15] in the transversity basis. The remaining $N^2 - N = N(N-1)$ observables are nondiagonal and thus composed of interference terms

$$\mathcal{O}^a_{\boldsymbol{nd}}(W,\theta) \propto \sum_{j,k} \boldsymbol{c}^a_{jk} b^*_j(W,\theta) b_k(W,\theta), \quad (47)$$

in this case for $a = 1,\ldots,N(N-1)$. The Hermitean matrices $\boldsymbol{c}^a_{jk}$ always render these observables to be either the real or imaginary parts of a particular linear combination of interference terms. For πN scattering, the spin-rotation parameters $\hat{R}$ and $\hat{A}$ are nondiagonal in the transversity basis [11,16], while for photoproduction the same is true for all double-polarization observables of type beam target, beam recoil, and target recoil [12,15].

Comparing the forms of the diagonal (46) and nondiagonal (47) observables, it is seen quickly that the former are generally always invariant under the N-fold rotations (44), while the latter are not. On the other hand, the one-fold rotations (45) leave both kinds of observables invariant. Therefore, for the spin reactions the interesting possibility emerges to obtain unique solutions in a TPWA once the energy-dependent overall phase has been fixed. The problem of such *complete experiments* in TPWAs for photoproduction has been explored before [5–7,12]. A very recent publication [17] treats the even more involved problem of electroproduction of pseudoscalar mesons. However, in these references the problem has not been formulated explicitly in the language involving rotations, which has been used in this work.

ACKNOWLEDGMENTS

The work of Y.W. and R.B. was supported in part by the Deutsche Forschungsgemeinschaft (SFB/TR16) and the European Community-Research Infrastructure Activity (FP7). A.Š. and L.T. are supported by the Deutsche Forschungsgemeinschaft (SFB 1044). The work of R.L.W. was supported through the US Department of Energy Grant No. DE-SC0016582.

APPENDIX A: ANSATZ FOR THE MINIMIZATION OF $W[F(x)]$ USING A DISCRETIZATION OF THE FUNCTION $F(x)$

In the following, we outline briefly a numerical alternative for the minimization of the functional (23) which, contrary to the method of Legendre expansions utilized in the main text, parametrizes the sought-after phase-rotation functions $F(x)$ by discretization on the interval $x \in [-1,1]$. Therefore, we introduce a set of equidistant points $\{x_n | n = 1,\ldots,N_I\}$ according to the prescription (30) used in the main text. The set of variables to be determined in the minimization procedure is given by the real and imaginary parts of the function $F(x)$ on this grid, i.e.,

$$r_n := \mathrm{Re}[F(x_n)], q_n := \mathrm{Im}[F(x_n)], n = 1,\ldots,N_I. \quad (A1)$$

These variables fulfill a similar purpose as the real and imaginary parts of the Legendre coefficients used in the method described in the main text, cf. Eq. (26). In order to minimize the quantity (23), the latter has first of all to be evaluated. Therefore, numerical integration has to be defined. We choose here the simplest possible way to do so and use the same grid employed in the discretization (A1). Therefore, any integral can be calculated using the form

$$\int_{-1}^{1} dx f(x) = \sum_{n=1}^{N_I} \Delta x\, f(x_n), \text{ using } \Delta x = \frac{2}{N_I}. \quad (A2)$$

It is seen that in order to obtain a precise knowledge of the solution function, as well as a small error in the numerical integration (A2), the number of grid points N_I has to be chosen as large as possible. In specific examples, we have had satisfactory results with numbers in the range $N_I = 250,\ldots,500$. Now, all ingredients necessary to formulate the functional (23) in the case of a minimization using the function discretization (A1) have been assembled. Again, the truncated nonrotated amplitude $A(x)$ is a known input. Numerical initial conditions for the parameters $\{q_n, r_n\}$ have to be drawn prior to fitting, for instance from the interval $[-1,1]$. An ensemble of initial parameter configurations should then be used, performing a functional minimization for each of them. One should employ ensembles of at least $N_{MC} = 200$ configurations. Omitting further intermediate steps, we quote the final result for the functional:

$$\begin{aligned} \boldsymbol{W}_{\mathrm{discr.}}(\{r_n, q_n\}) &:= \sum_{n=1}^{N_I} \left(r_n^2 + q_n^2 - 1\right)^2 + \left[\sum_{n=1}^{N_I} \Delta x \Big(r_n \mathrm{Im}[A(x_n)] + q_n \mathrm{Re}[A(x_n)]\Big)\right]^2 \\ &+ \sum_{k=1}^{K_{\mathrm{cut}}} \left\{\left[\sum_{n=1}^{N_I} \Delta x (r_n \mathrm{Re}[A(x_n)] - q_n \mathrm{Im}[A(x_n)]) P_{L+k}(x_n)\right]^2 + \left[\sum_{n=1}^{N_I} \Delta x (r_n \mathrm{Im}[A(x_n)] + q_n \mathrm{Re}[A(x_n)]) P_{L+k}(x_n)\right]^2\right\}. \quad (A3) \end{aligned}$$

Note that in this case, the parameters N_I and K_{cut} can be tuned independently from each other. This is different from the minimization scheme using Legendre expansions described in the main text, where the parameters $\mathcal{L}_{\mathrm{cut}}$ and K_{cut} have been connected. Using the minimization with the discretization functional (A3), we have obtained the same solutions as with the Legendre parametrization (32) for specific toy-model examples. However, the discretization method has proven to be the numerically more demanding and less stable of the two.

APPENDIX B: THE FUNCTIONAL $W[F(x)]$ AS AN ORDINARY FUNCTION $W(\{L_k\})$, DEPENDING ON LEGENDRE COEFFICIENTS

As hinted at in the main text, the minimization functional (23) becomes, once the phase-rotation function $F(x)$ is parametrized as a Legendre series, an ordinary function depending on the Legendre coefficients. Here, we derive a formal expression of the resulting functional, which is then for finite Legendre expansions equal to the form (32) used in our numerical minimizations. We assume here an initial nonrotated amplitude $A(W,\theta)$ truncated at L [i.e., the truncated version of Eq. (1)] and for the most general formal case, an infinite Legendre series for the phase-rotation function

$$F(x) = \sum_{k=0}^{\infty} L_k P_k(x). \tag{B1}$$

Now, all three terms appearing in the formal definition (23) of the minimization functional $\boldsymbol{W}[F(x)]$ are investigated with regard to their dependence on the complex Legendre coefficients $\{L_k\}$. The first term, i.e., the sum over x, in Eq. (23) imposes the unimodularity of $F(x)$. The squared modulus of the latter is appearing here, which under the present assumptions can be rewritten as follows:

$$\begin{aligned} |F(x)|^2 = F^*(x)F(x) &= \left(\sum_{k'=0}^{\infty} L_{k'}^* P_{k'}(x)\right)\left(\sum_{k=0}^{\infty} L_k P_k(x)\right) \\ &= \sum_{k,k'=0}^{\infty} L_{k'}^* L_k P_{k'}(x) P_k(x) = \sum_{k,k'=0}^{\infty} \sum_{m=|k'-k|}^{k'+k} L_{k'}^* L_k \langle k',0;k,0|m,0\rangle^2 P_m(x). \end{aligned} \tag{B2}$$

The term in the second line of Eq. (23) restricts the S wave to an overall phase constraint. The imaginary part which is squared there becomes

$$\begin{aligned} \mathrm{Im}\left[\int_{-1}^{1} dx\, F(x)A(x)\right] &= \mathrm{Im}\left[\int_{-1}^{1} dx \left(\sum_{k'=0}^{\infty} L_{k'} P_{k'}(x)\right)\left(\sum_{\ell=0}^{L} (2\ell+1) A_\ell P_\ell(x)\right)\right] \\ &= \mathrm{Im}\left[\sum_{k'=0}^{\infty}\sum_{\ell=0}^{L} L_{k'}(2\ell+1)A_\ell \int_{-1}^{1} dx\, P_{k'}(x)P_\ell(x)\right] = 2\,\mathrm{Im}\left[\sum_{k'=0}^{\infty}\sum_{\ell=0}^{L} L_{k'} A_\ell \delta_{k'\ell}\right] = 2\,\mathrm{Im}\left[\sum_{\ell=0}^{L} L_\ell A_\ell\right], \end{aligned} \tag{B3}$$

using just the basic orthogonality relation for the Legendre polynomials. Finally, the infinite sum over k in the third and fourth line of the definition (23) sets all the higher partial wave projections above L to zero. Every summand in this infinite series consist of the modulus squared of a complex projection integral. This integral can again be formulated explicitly as a function of $\{L_k\}$:

$$\begin{aligned} \int_{-1}^{1} dx\, F(x)A(x)P_{L+k}(x) &= \int_{-1}^{1} dx \left(\sum_{r=0}^{\infty} L_r P_r(x)\right)\left(\sum_{\ell=0}^{L}(2\ell+1)A_\ell P_\ell(x)\right) P_{L+k}(x) \\ &= \sum_{r=0}^{\infty}\sum_{\ell=0}^{L}(2\ell+1)A_\ell L_r \int_{-1}^{1} dx\, P_r(x)P_\ell(x)P_{L+k}(x) \\ &= \sum_{r=0}^{\infty}\sum_{\ell=0}^{L}\sum_{m=|\ell-L-k|}^{\ell+L+k} (2\ell+1)A_\ell L_r \langle \ell,0;L+k,0|m,0\rangle^2 \int_{-1}^{1} dx\, P_r(x)P_m(x) \\ &= 2\sum_{\ell=0}^{L}\sum_{m=|\ell-L-k|}^{\ell+L+k} \frac{(2\ell+1)}{(2m+1)} A_\ell L_m \langle \ell,0;L+k,0|m,0\rangle^2. \end{aligned} \tag{B4}$$

Combining the intermediate results (B2), (B3), and (B4), we arrive at the final expression for the minimization functional $\boldsymbol{W}$ as a function of the Legendre coefficients

$$\boldsymbol{W}(\{L_k\}) = \sum_x \left(\sum_{k,k'=0}^{\infty} \sum_{m=|k'-k|}^{k'+k} L_{k'}^* L_k \langle k',0;k,0|m,0\rangle^2 P_m(x) - 1 \right)^2 + \left(\sum_{\ell=0}^{L} \mathrm{Im}[L_\ell A_\ell] \right)^2$$
$$+ \sum_{k=1}^{\infty} \sum_{\ell,\tilde{\ell}=0}^{L} \sum_{m=|\ell-L-k|}^{\ell+L+k} \sum_{\tilde{m}=|\tilde{\ell}-L-k|}^{\tilde{\ell}+L+k} \frac{(2\ell+1)}{(2m+1)} \frac{(2\tilde{\ell}+1)}{(2\tilde{m}+1)} A_\ell^* L_m^* A_{\tilde{\ell}} L_{\tilde{m}} \langle \ell,0;L+k,0|m,0\rangle^2 \langle \tilde{\ell},0;L+k,0|\tilde{m},0\rangle^2. \quad \text{(B5)}$$

We note that this function is defined purely in terms of the information on the input amplitude, i.e., its truncation order L and partial waves A_ℓ. Clebsch-Gordan coefficients and the Legendre polynomials appearing here are known. Therefore, the only free parameters here are just the real and imaginary parts of the Legendre coefficients, as it should be. Furthermore, it should be noted that the expression (B5) is still quite formal, especially since it still contains an infinite sum over k. For practical numerical purposes, the infinite sum over the partial-wave projections, as well as the Legendre expansion (B1), would have to be truncated.

[1] J. E. Bowcock and H. Burkhardt, Rep. Prog. Phys. **38**, 1099 (1975).
[2] L. P. Kok., Ambiguities in Phase Shift Analysis, in *Delhi 1976, Conference on Few Body Dynamics* (North Holland, Amsterdam, 1976), pp. 43–46.
[3] D. Atkinson, L. P. Kok, M. de Roo, and P. W. Johnson, Nucl. Phys. B **77**, 109 (1974).
[4] J. H. Crichton, Nuovo Cimento A **45**, 256 (1966).
[5] R. L. Workman, L. Tiator, Y. Wunderlich, M. Döring, and H. Haberzettl, Phys. Rev. C **95**, 015206 (2017).
[6] Y. Wunderlich, R. Beck, and L. Tiator, Phys. Rev. C **89**, 055203 (2014).
[7] V. F. Grushin, in *Photoproduction of Pions on Nucleons and Nuclei*, edited by A. A. Komar (Nova Science, New York, 1989), p. 1ff.
[8] A. Švarc, Y. Wunderlich, H. Osmanović, M. Hadžimehmedović, R. Omerović, J. Stahov, V. Kashevarov, K. Nikonov, M. Ostrick, L. Tiator, and R. Workman, arXiv:1706.03211 [nucl-th].
[9] For the first identity, see, for instance, W. J. Thompson, *Angular Momentum* (John Wiley & Sons, New York, 2008). The second identity is a well-known relation between $3j$ symbols and Clebsch-Gordan coefficients.
[10] J.-P. Dedonder, W. R. Gibbs, and M. Nuseirat, Phys. Rev. C **77**, 044003 (2008).
[11] N. W. Dean and P. Lee, Phys. Rev. D **5**, 2741 (1972).
[12] A. S. Omelaenko, Sov. J. Nucl. Phys. **34**, 406 (1981).
[13] G. Keaton and R. Workman, Phys. Rev. C **54**, 1437 (1996).
[14] A. Gersten, Nucl. Phys. B **12**, 537 (1969).
[15] W. T. Chiang and F. Tabakin, Phys. Rev. C **55**, 2054 (1997).
[16] G. Höhler, *Pion Nucleon Scattering*, Part 2, Landolt-Börnstein: Elastic and Charge Exchange Scattering of Elementary Particles Vol. 9b (Springer-Verlag, Berlin, 1983).
[17] L. Tiator, R. L. Workman, Y. Wunderlich, and H. Haberzettl, Phys. Rev. C **96**, 025210 (2017).